Journal of Fluorescence, Vol. 9, No. 2, 1999

Photophysics and Fluorimetric Titrations of Fluorescent Ion Indicators

Noël Boens,[1,2] Els Cielen,[1] Kristof Van Werde,[1] and Frans C. De Schryver[1]

Received August 7, 1998; accepted November 11, 1998

A test based on time-resolved fluorescence experiments (*Anal. Biochem.***245**, 28–37, 1997) allows one to assess the interference of the excited-state association with the fluorimetric determination of the ground-state dissociation constant K_d of fluorescent ion:indicator complexes. If an inflection point occurs in the plot of the fluorescence signal *vs* − log[ion] in the ion concentration range where both decay times are invariant, this inflection point can be associated with the correct K_d. Here we apply this test to the fluorescent ion indicators SBFO (for Na^+), Mag-fura-2 (for Mg^{2+}), and APTRA-BTC (for Ca^{2+}). In all three cases the decay times are invariant in the concentration ranges of the respective ions where the fluorescence titrations show unique inflection points, indicating that the fluorimetrically determined K_d values are the true K_d values.

KEY WORDS: Fluorescence titration; fluorescent ion indicator; decay time analysis; Mag-fura-2; SBFO; APTRA-BTC.

INTRODUCTION

The measurement of intracellular ion concentrations is of the utmost importance in the fields of biology and medicine. Because of their inherently interesting properties, fluorescent indicators are the ideal tool for the nondestructive determination of intracellular Ca^{2+}, H^+, Na^+, K^+, and Mg^{2+} concentrations and their variations [1,2]. Therefore, fluorescent ion indicators continue to be the focus of intense research. Successful indicators must fulfill a series of criteria in addition to the chemically obvious ones of stability, specificity, and sensitivity. The major requirements for an indicator for intracellular ions are (i) an affinity that closely matches normal cytosolic concentrations for the specific ion, (ii) a selectivity for the intended ion over other ions present, (iii) an easily detectable change in the absorption (excitation) and/or emission properties upon binding of the ion of interest. The first condition presumes that the ground-state dissociation constant K_d of the ion:indicator complex is of the same order of magnitude as the ion concentration to be monitored. Hence, the correct determination of K_d is essential for any ion indicator.

Fluorescence spectroscopy is often used to evaluate the K_d of the formed complexes provided that the association–dissociation leads to a change in the measured steady-state fluorescence signal [3]. However, as the fluorescence signal depends on both ground-state and excited-state parameters, the fluorimetric determination of K_d is not as straightforward as by absorption spectrophotometry. It is not generally acknowledged that the excited-state reaction between indicator and ion may influence the value of K_d derived from fluorimetric titration. The degree of interference of the excited-state reaction with the fluorimetric determination of K_d depends on the values of the excited-state rate constants and/or the chosen excitation and emission wavelengths [3,4]. The rate constant values can be assessed by the single-step global compartmental analysis [5,6] of the fluorescence decay surface of an indicator as a function of the ion concentration.

[1] Department of Chemistry, Katholieke Universiteit Leuven, Celestijnenlaan 200F, 3001 Heverlee, Belgium.
[2] To whom correspondence should be addressed.

1053-0509/99/0600-0103$16.00/0 © 1999 Plenum Publishing Corporation

We have developed a test using measurements of time-resolved and steady-state fluorescence as a function of the ion concentration to assess the possible misevaluation of K_d via fluorimetric titration due to the excited-state reaction [4]. Here we apply this test to the commercial fluorescent indicators SBFO (for Na^+) [7,8], Mag-fura-2 (for Mg^{2+}) [7,9], and APTRA-BTC (for Ca^{2+}) [7].

SBFO is a commercially available fluorescent indicator [7] for the real-time determination of Na^+ concentrations. This sodium indicator consists of a diazacrown ether linked via its nitrogens to a benzofuran oxazole (Fig. 1A). The cavity size of the complex-forming group confers selectivity for Na^+. The K_d value of the Na^+:SBFO complex is 95 mM in the presence of physiological concentrations of K^+ and 50 mM without K^+ [8]. SBFO binds Na^+ with a 1:1 stoichiometry, inducing a threefold enhancement in fluorescence intensity and shifting the maxima of the excitation and emission spectra to shorter wavelengths. The fluorescence is relatively unaffected by changes in pH between 6.5 and 7.5.

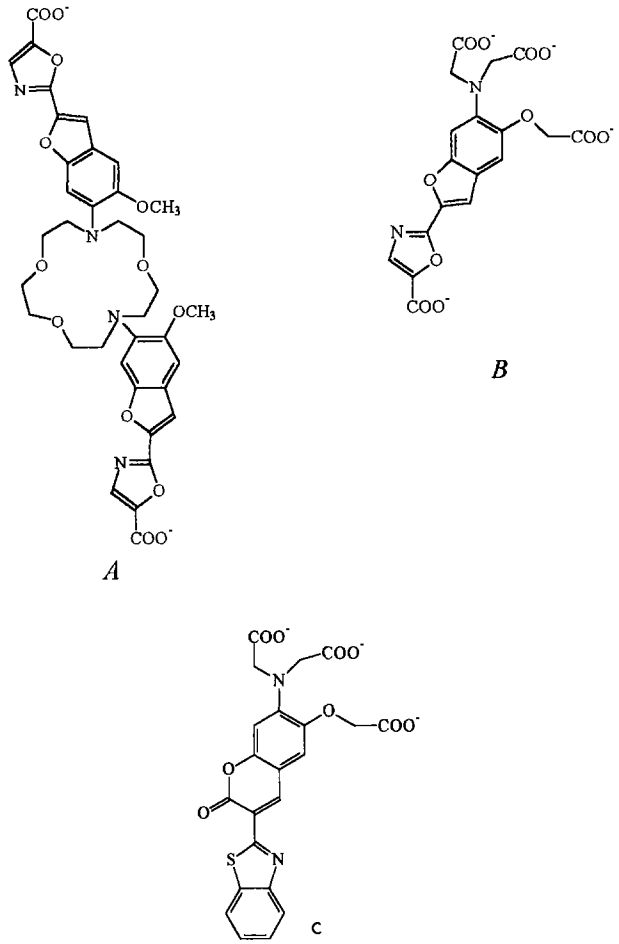

Fig. 1. Chemical structures of SBFO (A), Mag-fura-2 (B), and APTRA-BTC (C).

To investigate magnesium's role in cellular functions, several fluorescent indicators for measuring intracellular Mg^{2+} concentrations are now commercially available [7]. The first fluorescent Mg^{2+} indicator is Furaptra [9], which is often referred to as Mag-fura-2 (Fig. 1B), to denote the similarity of its structure and spectral response to those of the Ca^{2+} indicator Fura-2 [10]. The K_d of the Mg^{2+}:Mag-fura-2 complex is 1.5 mM, a value close to the cytosolic level of Mg^{2+}, which is typically between 0.1 and 6 mM [11,12]. Mag-fura-2 also binds Ca^{2+}; however, common physiological Ca^{2+} concentrations (10 nM–1 μM) do not usually interfere with Mg^{2+} measurements because the affinity of Mag-fura-2 for Ca^{2+} is low (the K_d of the Ca^{2+}:Mag-fura-2 complex is 53 μM, a value which is two or three orders of magnitude above the physiological Ca^{2+} concentration in most cells). The affinity of Mag-fura-2 for Mg^{2+} is reported [13] to be unchanged at pH values between 5.5 and 7.4 and temperatures between 22 and 37°C. Mag-fura-2 undergoes an appreciable shift in excitation wavelength upon Mg^{2+} binding [11,12]. The fluorescence of the indicator is relatively unaffected by changes in pH between 6.5 and 7.5 [11,12].

The coumarin benzothiazole-based APTRA-BTC (Fig. 1C) is a recent excitation–ratiometric fluorescent indicator for detecting low concentrations of Zn^{2+} in the presence of relatively high concentrations of Ca^{2+} or Mg^{2+} [7]. Because of the relatively weak binding of Zn^{2+} to APTRA-BTC (the K_d of the Zn^{2+}:APTRA-BTC complex is about 1.4 μM at pH 7.0 and 22°C) [7], this indicator may be more suitable for measuring Zn^{2+} in environmental samples than inside cells [the intracellular concentration of free Zn^{2+} is extremely low in most cells (< 1 nM)]. APTRA-BTC is derived from BTC [7], a ratiometric Ca^{2+} indicator with a moderate affinity for Ca^{2+} (the K_d of the Ca^{2+}:BTC complex is approximately 7 μM [7]). The low-affinity Ca^{2+} indicator BTC makes the accurate quantitative determination of high intracellular Ca^{2+} levels possible. Since the affinity of APTRA-BTC for Ca^{2+} is much lower than that of BTC, APTRA-BTC may be useful for sensing extracellular Ca^{2+} levels or monitoring Ca^{2+} in solutions or in extracts of environmental samples. Further details on the fluorescence of APTRA-BTC in the absence and presence of Ca^{2+} and Zn^{2+} will be reported elsewhere.

THEORY

Consider a system consisting of two distinct types of ground-state species and two corresponding types of

excited-state species. The kinetic model for such a system is presented in Scheme I. In the ground state the free form of the indicator, **1**, can undergo a reversible association with ion X to give the bound form, **2**, of the indicator. The association–dissociation is described by the ground-state dissociation constant K_d [Eq. (1)],

$$K_d = [1][X]/[2] \tag{1}$$

where figures in brackets denote molarities. It is assumed that only species **1** and **2**, which are in chemical equilibrium with each other, absorb light at the excitation wavelength λ^{ex}. Furthermore, the model depicted in Scheme I assumes a 1:1 stoichiometry between **1** and X. Excitation by light creates the excited-state species **1*** and **2***, which can decay by fluorescence (F) and nonradiative (NR) processes. The composite rate constants for those processes are denoted k_{01} ($=k_{F1} + k_{NR1}$) and k_{02} ($=k_{F2} + k_{NR2}$). The second-order rate constant describing the association **1*** + X $\rightarrow$ **2*** is represented by k_{21}. The first-order rate constant for the dissociation of **2*** into **1*** and X is described by k_{12}.

Kinetics

If the system shown in Scheme I is excited with a δ-pulse which does not significantly alter the concentrations of the ground-state species (i.e., in the low excitation limit), the fluorescence decays are dual exponential [14],

$$f(\lambda^{ex}, \lambda^{em}, t) = \alpha_1 \exp(-t/\tau_1) + \alpha_2 \exp(-t/\tau_2), \quad t \geq 0 \tag{2}$$

where the amplitudes α_i depend on all the rate constants k_{ij}, the ground-state dissociation constant K_d, the concentration of X, and, additionally, λ^{em} and λ^{ex}. The decay times τ_i [Eq. (3)], however, depend exclusively on k_{ij} and [X].

$$(\tau_{1,2})^{-1} = 1/2\ \{S_1 + S_2 \mp [(S_1 - S_2)^2 + 4k_{12}\, k_{21}\, [X]]^{1/2}\} \tag{3a}$$

with

$$S_1 = k_{01} + k_{21}\,[X] \tag{3b}$$

$$S_2 = k_{02} + k_{12} \tag{3c}$$

For clarity, we do not use the notation $\tau_{1,2}$ but we refer to τ_S (S for short) and τ_L (L for long).

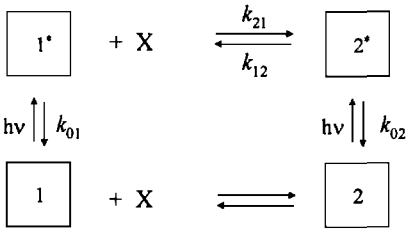

Scheme I

Fluorimetric Titration

If the system depicted in Scheme I is excited with light of constant intensity, and if the absorbance of the sample is less than 0.1, the measured steady-state fluorescence signal $F(\lambda^{ex}, \lambda^{em}, [X])$ observed at λ^{em} due to excitation at λ^{ex} is given by [3,4]

$$F(\lambda^{ex}, \lambda^{em}, [X]) = \frac{\epsilon_1(\lambda^{ex})a_1\,(\lambda^{em}, [X])K_d + \epsilon_2(\lambda^{ex})a_2(\lambda^{em}, [X])\,[X]}{K_d + [X]} C_T\psi\,(\lambda^{ex}, \lambda^{em}) \tag{4}$$

where $\epsilon_i(\lambda^{em})$ represents the molar extinction coefficient of species i at λ^{em}. The coefficients a_i are given by [3,4]

$$a_1(\lambda^{em}, [X]) = \frac{(k_{02} + k_{12})c_1(\lambda^{em}) + k_{21}[X]c_2(\lambda^{em})}{k_{01}(k_{02} + k_{12}) + k_{02}k_{21}[X]} \tag{5a}$$

$$a_2(\lambda^{em}, [X]) = \frac{k_{12}c_1(\lambda^{em}) + (k_{01} + k_{21}\,[X])c_2\,(\lambda^{em})}{k_{01}(k_{02} + k_{12}) + k_{02}k_{21}[X]} \tag{5b}$$

The emission weighting factors $c_i(\lambda^{em})$ are defined as [6]

$$c_i(\lambda^{em}) = k_{Fi} \int_{\Delta\lambda^{em}} \rho_i(\lambda^{em})\, d\lambda^{em} \tag{6}$$

k_{Fi} represents the fluorescence rate constant of species i^*, $\Delta\lambda^{em}$ is the emission wavelength interval around $\delta\lambda^{em}$ where the fluorescence signal is monitored, and $\rho_i(\lambda^{em})$ is the steady-state fluorescence spectrum of species i^* normalized to unity.

The factor $\psi(\lambda^{ex}, \lambda^{em})$ includes instrumental parameters,

$$\psi(\lambda^{ex}, \lambda^{em}) = 2.3dI_0\,(\lambda^{ex})\,\xi(\lambda^{em}) \tag{7}$$

where d denotes the excitation light path, $I_0(\lambda^{ex})$ represents the intensity of the exciting light at λ^{ex} impinging on the sample, and $\xi(\lambda^{em})$ is a factor taking into account the efficiency of both the optics and the detector.

C_T is the total analytical concentration of the fluorescent indicator:

$$C_T = [1] + [2] \tag{8}$$

In general the plot of F *vs* $-\log[X]$ exhibits multiple inflections, one of which will correspond to K_d.

If the product k_{21} [X] describing the association of **1*** with X is negligible within the range of used [X], the decay times τ_i [Eq. (3)] and the coefficients a_i [Eq. (5)] become practically independent of [X]. The latter are then given by [4]

$$a_1(\lambda^{em}) = c_1(\lambda^{em})/k_{01} \tag{9a}$$

$$a_2(\lambda^{em}) = \frac{k_{12}c_1(\lambda^{em}) + k_{01}c_2(\lambda^{em})}{k_{01}(k_{02} + k_{12})} \tag{9b}$$

In this case the plot of F *vs* $-\log[X]$ starts at $F_{min} = \epsilon_1(\lambda^{ex})a_1(\lambda^{em})C_T\psi(\lambda^{ex}, \lambda^{em})$ for very low [X]. It rapidly changes around the unique inflection at $-\log[X] = pK_d$ and then asymptotically approaches $F_{max} = \epsilon_2(\lambda^{ex})a_2(\lambda^{em})C_T\psi(\lambda^{ex}, \lambda^{em})$ for very high [X]. F_{min} and F_{max} thus represent the fluorescence signals of the free and bound forms of the indicator, respectively.

If k_{21} [X] ≈ 0, Eq. (4) can be rewritten as

$$F = \frac{K_dF_{min} + [X]F_{max}}{K_d + [X]} \tag{10}$$

This equation allows one to determine K_d from a fluorimetric titration as a function of [X]. Conversely, once K_d is known, Eq. (10) can be used to determine the unknown [X]. This equation requires that F, F_{min}, and F_{max} all be determined at the same instrumental sensitivity, excitation intensity and optical path length [i.e., same $\psi(\lambda^{ex}, \lambda^{em})$], and total concentration of indicator (same C_T). Equation (10) is often rearranged in the form of a Hill plot:

$$\log[(F - F_{min})/(F_{max} - F)] = \log[X] - \log K_d \tag{11}$$

The expression on the left side of Eq. (11) plotted *vs* log[X] should give a straight line which intersects the abscissa at the value corresponding to $\log K_d$.

When $k_{21}[X] \approx 0$ the decay times $\tau_{S,L}$ [Eq. (3)] are invariant with [X] and correspond to $1/k_{01}$ and $1/(k_{02} + k_{12})$.

A relatively simple experimental test based on time-resolved and steady-state fluorescence measurements can be used to assess the possible misevaluation of K_d from fluorimetric titrations due to the excited-state reaction. If both decay times τ_i [Eq. (3)] are constant over the used concentration range of X, the contribution of the term $k_{21}[X]$ is small enough to make the coefficients a_i [Eq. (5)] virtually independent of [X] [see Eq. (9)], and the plot of F *vs* $-\log[X]$ will have a unique inflection at $-\log[X] = pK_d$. Collecting fluorescence decay traces in the same X concentration range as used in the fluorimetric titration and analyzing them simultaneously (10,11) as biexponentials with linked decay times allows one to check the invariance of the decay times. As [X] becomes larger, the contribution of the term $k_{21}[X]$ is not negligible any longer, resulting in changing decay times and making the coefficients a_i dependent on [X], possibly causing an additional inflection point in the fluorimetric titration curve. Therefore, the inflection point(s) in the [X] range where the decay times vary cannot be attributed to ground-state dissociation.

EXPERIMENTAL

Materials

The experimental details for SBFO [15] and Mag-fura-2 [16] have already been published. Therefore, only experimental conditions for APTRA-BTC are explicitly given. APTRA-BTC tripotassium salt (cell impermeant) was obtained from Molecular Probes (Eugene, OR). MOPS [3-(*N*-morpholino)propanesulfonic acid] free acid (>99.5%) was purchased from Sigma Chemie (Bornem, Belgium). KCl (99.99+%) and $CaCl_2$ (99.99+%) were obtained from Aldrich Chimica (Geel, Belgium). All products were used as received. Fluorimetric measurements were performed using aqueous buffer solutions at pH 7.2 of (i) SBFO and NaCl, (ii) Mag-fura-2 and $MgCl_2$, and (iii) APTRA-BTC and $CaCl_2$. Milli-Q water was used to prepare the buffer solutions. To obtain the required pH for the SBFO measurements, solutions of NaOH and MOPS were used; for the Mag-fura-2 measurements, solutions of Tris and HCl; and for the APTRA-BTC measurements, solutions of KOH and MOPS. The ionic strength of solutions with different $[Na^+]$ or $[Mg^{2+}]$ varied, while that of solutions with different $[Ca^{2+}]$ was kept constant by the addition of KCl. All measurements were carried out at 20°C (SBFO and Mag-fura-2) or 22°C (APTRA-BTC).

Instrumentation

Fully corrected steady-state excitation and emission spectra were recorded on a SPEX Fluorolog 212.

Fluorescence decay traces were collected by the single-photon timing technique [17,18] using the synchrotron radiation facility SUPER-ACO (Anneau de Collision d'Orsay at LURE, France) as described elsewhere [19]. The storage ring provided vertically polarized light

pulses with a full width at half-maximum of ≃500 ps at a frequency of 8.33 MHz in the double-bunch mode. A Hamamatsu microchannel plate R1564U-06 was utilized to detect the fluorescence photons under the magic angle (54°44′). The instrument response function was determined by measuring the light scattered by glycogen in aqueous solution at the emission wavelength. All decay traces were collected in 1K channels of a multichannel analyzer and contained approximately 5×10^3 peak counts. The time increment per channel was 21.4 ps for the SBFO measurements, 5.8 ps for Mag-fura-2, and 32 ps for APTRA-BTC.

Data Analysis

The global compartmental analysis of the fluorescence decay surface of species undergoing excited-state processes was implemented in the existing general global analysis program [20] based on Marquardt's [21] algorithm. A detailed description of the global compartmental analysis program can be found in Ref. 4. Using this approach, all decay traces collected at different excitation/emission wavelengths and at different [X] are linked by the rate constants k_{01}, k_{21}, k_{02}, k_{12} defining the system and can therefore be analyzed simultaneously.

The fitting parameters were determined by minimizing the global reduced chi-square χ^2_g.

$$\chi^2_g = \sum_{l}^{q} \sum_{i} w_{li}(y^o_{li} - y^c_{li})^2/\nu \qquad (18)$$

where the index l sums over q experiments, and the index i sums over the appropriate channel limits for each individual experiment. y^o_{li} and y^c_{li} denote, respectively, the experimentally measured (observed) and fitted (calculated) values corresponding to the ith channel of the lth experiment. w_{li} is the corresponding statistical weight. ν represents the number of degrees of freedom for the entire multidimensional fluorescence decay surface. χ^2_g and its corresponding $Z_{\chi^2_g}$ [Eq. (19)] provide numerical goodness-of-fit criteria for the entire fluorescence decay surface.

$$Z_{\chi^2_g} = (\chi^2_g - 1)(1/2\ \nu)^{1/2} \qquad (19)$$

Using $Z_{\chi^2_g}$ the goodness-of-fit of analyses with different ν can be readily compared. The additional statistical criteria to judge the quality of the fit comprised both graphical and numerical tests and are described elsewhere [18]. Standard error estimates were obtained from the parameter covariance matrix available from the nonlinear least-squares analysis. All quoted errors are 1 standard deviation. All analyses were performed on an IBM RISC System/6000 computer.

APPLICATION TO FLUORESCENT ION INDICATORS

In this section we apply the new test [4] to the fluorescent ion indicators SBFO, Mag-fura-2, and APTRA-BTC. For all indicators steady-state fluorimetric titrations were performed. Additionally, fluorescence decay traces were collected as a function of [X] and described by simultaneous biexponential analysis [22,23]. Furthermore, the decays of SBFO and Mag-fura-2 were analyzed by global compartmental analysis [5,6] yielding estimates for the rate constants k_{01}, k_{21}, k_{02}, k_{12}.

SBFO + Na^+

K_d of the Na^+:SBFO complex was determined from a Hill plot [Eq. (11)] using the steady-state fluorescence signal F(340 nm, 500 nm) at 20°C, pH 7.2, in aqueous solution in the absence of K^+ (Fig. 2). The linear Hill plot (with correlation coefficient 0.998) yielded a value of 34 mM for K_d ($pK_d = 1.47 \pm 0.05$) and indicated a 1:1 stoichiometry for the Na^+:SBFO complex. The pK_d value is reasonably close to that estimated by Minta and Tsien ($pK_d = 1.30$) [8].

Decay traces of SBFO at different [Na^+] ranging from 2.68 mM to 4.18 M were monitored at three sets of excitation/emission wavelengths: (i) $\lambda^{ex} = 340$ nm, $\lambda^{em} = 500$ nm; (ii) $\lambda^{ex} = 340$ nm, $\lambda^{em} = 510$ nm; and (iii) $\lambda^{ex} = 355$ nm, $\lambda^{em} = 510$ nm.

The decay traces of solutions with identical Na^+ concentrations were analyzed globally as biexponential functions [Eq. (2)] with the decay times linked over the excitation and emission wavelengths at each [Na^+]. Biexponential analyses gave good fits at each Na^+ concentration. However, the variation of τ_S as a function of

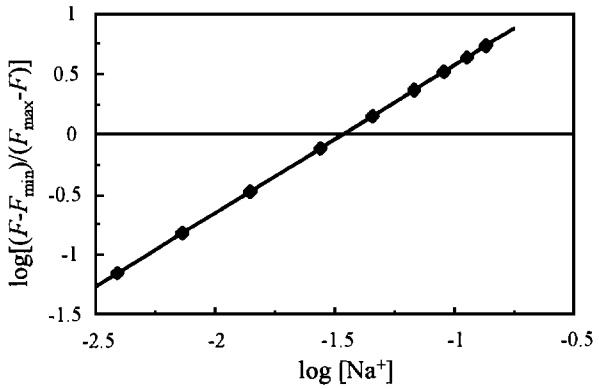

Fig. 2. Hill plot constructed with the steady-state fluorescence signals F(340 nm, 500 nm) of SBFO *vs* log[Na^+] at pH 7.2 in aqueous K^+ free solution at 20°C.

Table I. Rate Constant Values (± SD) of SBFO Estimated by Global Compartmental Analysis[a]

Rate constant	
k_{01} $(ns)^{-1}$	0.465 (±0.001)
k_{21} $(M\ ns)^{-1}$	0.087 (±0.004)
k_{02} $(ns)^{-1}$	0.537 (±0.002)
k_{12} $(ns)^{-1}$	0.127 (±0.002)

[a] Values taken from Meuwis *et al.* [15]

$-\log[Na^+]$ was erratic, due to the negligible values of the preexponential values associated with the short decay times τ_S [15,23]. Furthermore, varying the excitation and emission wavelengths as done experimentally in the collection of the decays hardly changes the preexponential factors, resulting in poor τ_S estimates [15,23]. Moreover, global biexponential analysis of simulated decay traces confirmed that accurate estimates were found only for τ_L and not for τ_S and the corresponding amplitudes [15].

In global compartmental analysis all (46) decay traces were simultaneously analyzed, yielding the rate constant values shown in Table I. Using these rate constant values the decay times were calculated as a function of $[Na^+]$ according to Eq. (3). Those decay time values are shown as solid lines in Fig. 3.

The global biexponential analysis with τ_L freely adjustable and with τ_S held fixed at the value calculated according to Eq. (3) using the rate constant values of Table I, yields the decay time values plotted in Fig. 3. The agreement between the τ_L values estimated by this global biexponential analysis and those computed according to Eq. (3) using the rate constant values in Table I is excellent. The decrease in τ_L with increasing $[Na^+]$ indicates that $k_{01} < k_{02}$ [24] and was confirmed by the results shown in Table I. Comparing Figs. 2 and 3 shows that both decay times are independent of $[Na^+]$ in the $[Na^+]$ range where the fluorimetric titration was performed (*i.e.*, where $-\log[Na^+]$ has a value between 0.8 and 2.4). Hence, in this $[Na^+]$ range the term $k_{21}[Na^+]$ is negligible so that a reliable K_d estimate is obtained from the Hill plot.

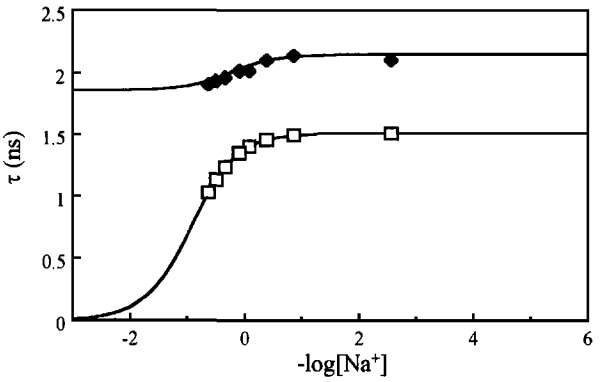

Fig. 3. Decay times τ_i (——) of SBFO as a function of $-\log[Na^+]$ calculated according to Eq. (3) using the rate constant values obtained from global compartmental analysis (Table I). The symbols (♦) represent τ_L estimated by global biexponential analysis at each $[Na^+]$ in which τ_S (□) was held fixed at the value calculated according to Eq. (3) using the rate constant values in Table I.

Mag-fura-2 + Mg^{2+}

The ground-state dissociation constant K_d of the Mg^{2+}:Mag-fura-2 complex can be estimated from a Hill plot [Eq. (11)] using the steady-state fluorescence signal F(340 nm, 500 nm) at 20°C and pH 7.2 (Fig. 4). The Hill plot gave a value of 1.78 mM for K_d (pK_d = 2.750 ± 0.003) and was consistent with a 1:1 stoichiometry (slope = 1.13 ± 0.04) for the Mg^{2+}:Mag-fura-2 complex. The K_d value is in good correspondence with that (1.5 mM) obtained by Raju *et al.* [9].

To determine the rate constants k_{01}, k_{21}, k_{02}, k_{12} fluorescence decays of Mag-fura-2 at 10 concentrations of Mg^{2+} up to 750 mM were measured at three sets of excitation/emission wavelengths: (i) λ^{ex} = 340 nm, λ^{em} = 490 nm; (ii) λ^{ex} = 340 nm, λ^{em} = 510 nm; and (iii) λ^{ex} = 370 nm, λ^{em} = 510 nm.

The decays collected from solutions with identical Mg^{2+} concentrations were analyzed globally as biexponential functions [Eq. (2)] with the decay times being linked over the emission and excitation wavelengths at each $[Mg^{2+}]$. Good-quality fits were obtained over the whole Mg^{2+} concentration range. The estimated decay times are shown in Fig. 5. The fact that both τ_L and τ_S decrease with increasing $[Mg^{2+}]$ indicates that $k_{01} < k_{02}$. [24]

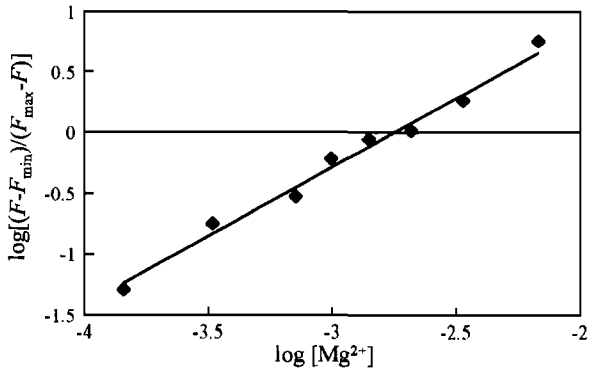

Fig. 4. Hill plot constructed with the steady-state fluorescence signals F(340 nm, 500 nm) of Mag-fura-2 *vs* $\log[Mg^{2+}]$ at pH 7.2 in aqueous solution at 20°C.

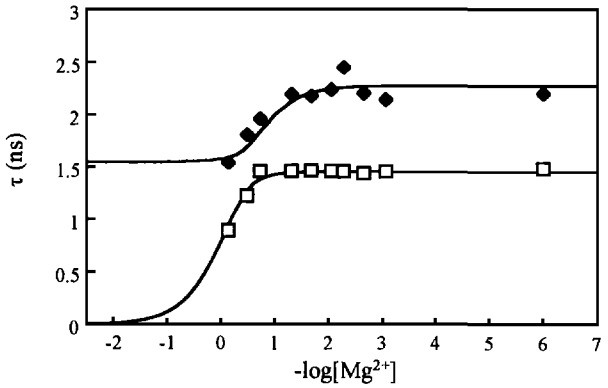

Fig. 5. Decay times τ_L (♦) and τ_S (□) of Mag-fura-2 as a function of $-\log[Mg^{2+}]$ estimated by global biexponential analysis at each $[Mg^{2+}]$. The solid lines represent the decay times calculated according to Eq. (3) using the rate constant values in Table II.

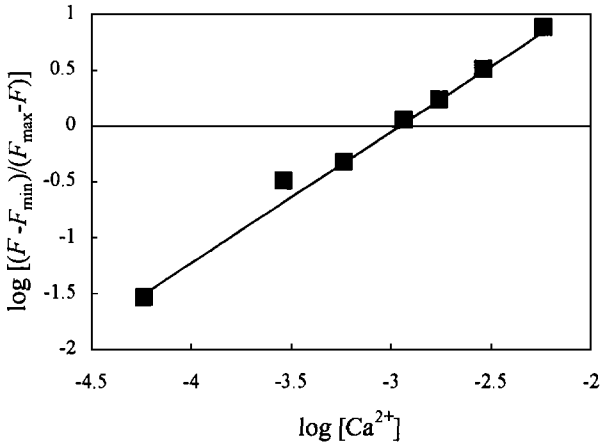

Fig. 6. Hill plot constructed with the steady-state fluorescence signals F(467 nm, 530 nm) of APTRA-BTC *vs* $\log[Ca^{2+}]$ at pH 7.2 in aqueous solution at 22°C.

In global compartmental analysis all the decay traces were analyzed simultaneously, resulting in the rate constants shown in Table II. Using these values the decay times $\tau_{S,L}$ can be calculated as a function of $[Mg^{2+}]$ according to Eq. (3). These decay times are plotted in Fig. 5 as a function of $-\log[Mg^{2+}]$ together with the decay times estimated directly from global biexponential analysis. There is an excellent agreement between both sets of decay times. Since both decay times are constant in the region where F vs $-\log[Mg^{2+}]$ exhibits the unique inflection, it can be attributed to K_d [4,14]. Fluorimetric titrations of Mag-fura-2 can thus be used to estimate the value of K_d correctly.

APTRA-BTC + Ca^{2+}

The K_d of the Ca^{2+}:APTRA-BTC complex was determined from a Hill plot [Eq. (11)] using the steady-state fluorescence signal F(467 nm, 530 nm) at 22°C, pH 7.2, in aqueous solution in the absence of Mg^{2+} (Fig. 6): The linear Hill plot (with correlation coefficient 0.958) yielded a value of 0.84 mM for K_d (pK_d = 3.1 ± 0.3) and indicated a 1:1 stoichiometry (slope = 1.06 ± 0.09)

Table II. Rate Constant Values (±SD) of Mag-fura-2 Estimated by Global Compartment Analysis[a]

Rate constant	
k_{01} $(ns)^{-1}$	0.439 (±0.003)
k_{21} $(M\ ns)^{-1}$	0.77 (±0.01)
k_{02} $(ns)^{-1}$	0.645 (±0.001)
k_{12} $(ns)^{-1}$	0.037 (±0.001)

[a] Values taken from Meuwis *et al.* [16].

for the Ca^{2+}:APTRA-BTC complex. The very low affinity of APTRA-BTC for Ca^{2+} makes this indicator unsuitable for sensing intracellular Ca^{2+} levels. However, extracellular Ca^{2+} concentrations can be quantified and Ca^{2+} in solutions or in extracts of environmental samples may be monitored with APTRA-BTC.

Eight decay traces of APTRA-BTC at different $[Ca^{2+}]$ ranging from 29.1 μM to 0.918 M were collected at 520 nm with excitation at 380 nm. Each decay trace was analyzed separately as a dual-exponential function [Eq. (2)], yielding good fits at each Ca^{2+} concentration (Fig. 7). Since the decay times seem to be independent of the free Ca^{2+} concentration, all eight decay traces were simultaneously analyzed as biexponentials, giving excellent fits. The estimated decay times were found to

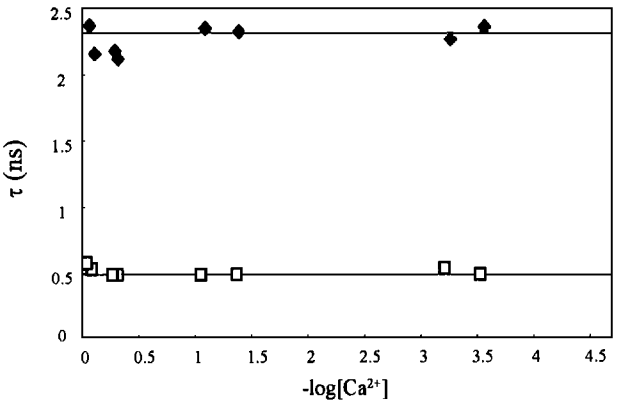

Fig. 7. Decay times τ_L (♦) and τ_S (□) of APTRA-BTC as a function of $-\log[Ca^{2+}]$ estimated by biexponential single-curve analysis at each $[Ca^{2+}]$. The solid lines represent the decay times estimated by global biexponential analysis of all eight decays collected over the entire Ca^{2+} concentration range.

be τ_S = 0.49 + 0.02 ns and τ_L = 2.34 + 0.01 ns. These decay time values are shown as solid lines in Fig. 7.

Comparison of Figs. 6 and 7 shows that τ_S and τ_L are independent of $[Ca^{2+}]$ in the concentration range where the fluorimetric titration was performed (i.e., from 14 μM to 11.6 mM). Hence, the unique inflection point in the fluorimetric titration can be attributed to K_d.

CONCLUSIONS

We have shown that it is possible to check by time-resolved fluorescence experiments whether the association reaction in the excited state interferes with the determination of K_d. If an inflection of the fluorimetric titration curve occurs in the ion concentration range where both decay times are invariant, this inflection point can be associated with the true pK_d. Since for each of the ion indicators (SBFO + Na^+, Mag-fura-2 + Mg^{2+}, and APTRA-BTC + Ca^{2+}), the inflection point in the fluorimetric titration curve occurs in the ion concentration range where the decay times are invariant, the interference of the excited state association with the fluorimetric determination of K_d can be neglected.

ACKNOWLEDGMENTS

N.B. is an *Onderzoeksdirecteur* and E.C. is an *Aspirant* of the *Fonds voor Wetenschappelijk Onderzoek (FWO)*. The authors thank M. Ameloot (LUC, Diepenbeek, Belgium), J. Gallay (LURE, Orsay, France), A. Kowalczyk (Nicholas Copernicus University, Torum, Poland), K. Meuwis (K. U. Leuven, Belgium), and M. Vincent (LURE, Orsay, France) for their contributions to this paper. The financial support of the *DWTC* through IUAP-4-11 is gratefully acknowledged.

REFERENCES

1. (a) A. W. Czamik (Ed.) (1992) *Fluorescent Chemosensors for Ion and Molecule Recognition*, ACS Symposium Series 538, American Chemical Society, Washington, DC. (b) J. R. Lakowicz (Ed.) (1994) *Topics in Fluorescence Spectroscopy, Vol. 4: Probe Design and Chemical Sensing*, Plenum Press, New York. (c) J.-P. Desvergne and A. W. Czarnik (Eds.) (1997) *Chemosensors for Ion and Molecule Recognition*, NATO ASI Series C 492, Kluwer Academic, Dordrecht.
2. (a) R. Y. Tsien (1989) in D. L. Taylor and Y.-L. Wang (Eds.), *Methods in Cell Biology, Vol. 30*, Academic Press, San Diego, pp. 127–156. (b) R. Y. Tsien (1991) *Annu. Rev. Neurosci.* **12**, 227–253.
3. A. Kowalczyk, N. Boens, V. Van den Bergh, and F. C. De Schryver (1994) *J. Phys. Chem.* **98**, 8585–8590.
4. A. Kowalczyk, N. Boens, K. Meuwis, and M. Ameloot (1997) *Anal. Biochem.* **245**, 28–37.
5. J. M. Beechem, M. Ameloot, and L. Brand (1985) *Chem. Phys. Lett.* **120**, 466–472.
6. M. Ameloot, N. Bones, R. Andriessen, V. Van den Bergh, and F. C. De Schryver (1991) *J. Phys. Chem.* **95**, 2041–2047.
7. R. P. Haugland (1996) in M. T. Z. Spence (Ed.), *Handbook of Fluorescent Probes and Research Chemicals, 6th ed.*, Molecular Probes, Eugene, OR, pp. 503–540, 572–577.
8. A. Minta and R. Y. Tsien (1989) *J. Biol. Chem.* **264**, 19449–19475.
9. B. Raju, E. Murphy, L. A. Levy, R. D. Hall, and R. E. London (1989) *Am. J. Physiol.* **256**, C540.
10. G. Grynkiewicz, M. Poenie, and R. Y. Tsien (1985) *J. Biol. Chem.* **160**, 3440.
11. J. Robbins, R. Cloues, and D. A. Brown (1992) *Pflügers Arch.* **420**, 347.
12. E. Heinonen and K. E. O. Åkerman (1987) *Biochim. Biophys. Acta* **898**, 331.
13. F. A. Lattanzio and D. K. Bartschat (1991) *Biochem. Biophys. Res. Commun.* **177**, 184.
14. J. B. Birks (1970) *Photophysics of Aromatic Molecules*, Wiley, New York.
15. K. Meuwis, N. Boens, F. C. De Schryver, M. Ameloot, J. Gallay, and M. Vincent (1998) *J. Phys. Chem. B* **102**, 641–648.
16. K. Meuwis, N. Boens, J. Gallay, and M. Vincent (1998) *Chem. Phys. Lett.* **287**, 412–420.
17. D. V. O'Connor and D. Phillips (1984) *Time-Correlated Single Photon Counting*, Academic Press, London.
18. N. Boens (1991) in W. R. G. Baeyens, D. De Keukeleire, and K. Korkidis (Eds.), *Luminescence Techniques in Chemical and Biochemical Analysis*, Dekker, New York, pp. 21–45.
19. O. P. Kuipers, M. Vincent, J. C. Brochon, H. M. Verheij, G. H. De Haas, and J. Gallay (1991) *Biochemistry* **30**, 8771–8785.
20. N. Boens, L. D. Janssens, and F. C. De Schryver (1989) *Biophys. Chem.* **33**, 77–90.
21. D. W. Marquardt. (1963) *J. Soc. Indust. Appl. Math.* **11**, 431–441.
22. J. R. Knutson, J. M. Beechem, and L. Brand (1983) *Chem. Phys. Lett.* **102**, 501–507.
23. L. D. Janssens, N. Boens, M. Ameloot, and F. C. De Schryver (1990) *J. Phys. Chem.* **94**, 3564–3576.
24. V. Van den Bergh, A. Kowalczyk, N. Boens, and F. C. De Schryver (1994) *J. Phys. Chem.* **98**, 9503–9508.